Jpn. J. Appl. Phys. Vol. 38 (1999) pp. 3120–3123
Part 1, No. 5B, May 1999

Pressure Sensitivity of a Fiber-Optic Microprobe for High-Frequency Ultrasonic Field

Yasuto UNO and Kentaro NAKAMURA
Precision and Intelligence Laboratory, Tokyo Institute of Technology, 4259 Nagatsuta, Midori-ku, Yokohama 226-8503, Japan

(Received November 28, 1998; accepted for publication January 29, 1999)

An acoustic microprobe is required to measure high-frequency ultrasonic fields with good spatial resolution. An optical fiber microprobe was proposed in our previous study, which consists of a small optical cavity 100 μm long made at the end of the fiber. The optical path length of the cavity is changed by the applied acoustic field, and the modulation of output light intensity is monitored at the other end of the fiber to derive information of the acoustic field. In the present study, the pressure sensitivity of the fiber-optic microprobe is discussed theoretically and experimentally. Mechanical deformation of the optical cavity by acoustic pressure is calculated by the finite element method (FEM), and the effect of the deformation on the optical property is analyzed for a low finesse microcavity.

KEYWORDS: fiber-optic microprobe, high-frequency ultrasonic field, Fabry-Perot resonator, pressure sensitivity, dynamic range, finite element method

1. Introduction

The recent rapid development of high-frequency ultrasonic engineering has given rise to the requirement of a miniature ultrasonic probe. Sensors should be smaller than the wavelength of ultrasound to be measured (less than several hundred μm) to realize high spatial resolution and to prevent interference with the ultrasonic field. It should also be able to withstand both intense sound pressure and high-level electromagnetic noise. An optical fiber sensor can overcome all of these problems. A fiber-optic probe with moderate sensitivity and a three-dimensionally confined sensing part, created by introducing a microcavity at the end of the fiber, has been proposed.[1,2] The optical path length of the cavity is varied by the applied acoustic field, and the modulation of output light intensity monitored at the other end of the fiber provides information of the acoustic field. We have also proposed a microprobe array for multipoint measurements.[3] Methods of predicting pressure sensitivity and dynamic range are needed for quantitative measurements and nonlinear ultrasonic field measurements. In this paper we describe the analysis of pressure sensitivity and dynamic range of the microprobe. Optical sensitivity to a deformation cavity is expressed by the Fabry-Perot equation and mechanical sensitivity to pressure is calculated by the finite element method (FEM). Then, the theoretical results of pressure sensitivity and dynamic range are compared with the experimental data of prototypes.

2. Construction and Principle of the Microprobe

Figure 1 shows the configuration of the probe to be discussed in this paper. A small dielectric polymer with refractive index n is attached to the fiber end through a half-mirror of reflectivity R. The other end of the cylinder is terminated with a full reflection mirror. The length of the cavity L is almost as large as the diameter of the fiber's cladding. Optical path nL of the cavity is changed due to the mechanical deformation or the refractivity change by acoustic pressure, and the sound wave can be measured by monitoring the reflected light I from the fiber end, if a monochromatic light is used and its wavelength is set at the slope of the cavity resonance. The reflectivity of a Fabry-Perot resonator is given by[4]

$$G_{\mathrm{R}} = \frac{(\sqrt{R} - G_{\mathrm{s}})^2 + 4\sqrt{R}G_{\mathrm{s}}\sin^2(2\pi nL/\lambda)}{(1 - \sqrt{R}G_{\mathrm{s}})^2 + 4\sqrt{R}G_{\mathrm{s}}\sin^2(2\pi nL/\lambda)}, \qquad (2.1)$$

where, G_{R} is the normalized reflected light intensity, G_{s} is the single-pass gain and λ is the light wavelength. The pressure sensitivity and the dynamic range of the proposed probe are determined by the sharpness and width of the Fabry-Perot resonance, respectively. Therefore, the relationship between sensitivity and dynamic range has a trade-off. Equation (2.1) includes information regarding the sharpness or the width of the Fabry-Perot resonance, which is called Finesse F:

$$F = \frac{4\sqrt{R}G_{\mathrm{s}}}{\left(1 - \sqrt{R}G_{\mathrm{s}}\right)^2}. \qquad (2.2)$$

In our prototypes, R and G_{s} are equal to 0.8–0.95 and 0.9–0.95, respectively, and F is 10–1000.

3. Analysis of the Pressure Sensitivity and the Dynamic Range

3.1 General description

The pressure sensitivity to be calculated here is defined as the ratio of the change in the reflected light ΔG_{R} to that in the applied sound pressure Δp, and is given by,

$$\frac{\Delta G_{\mathrm{R}}}{\Delta p} = \frac{\Delta(nL)}{\Delta p}\frac{\Delta G_{\mathrm{R}}}{\Delta(nL)}. \qquad (3.1)$$

Here, $\Delta(nL)/\Delta p$ shows the pressure sensitivity of the optical path nL, while $\Delta G_{\mathrm{R}}/\Delta(nL)$ describes the gradient of the optical resonance curve with respect to the optical path. The former can be understood by the analysis of mechanical

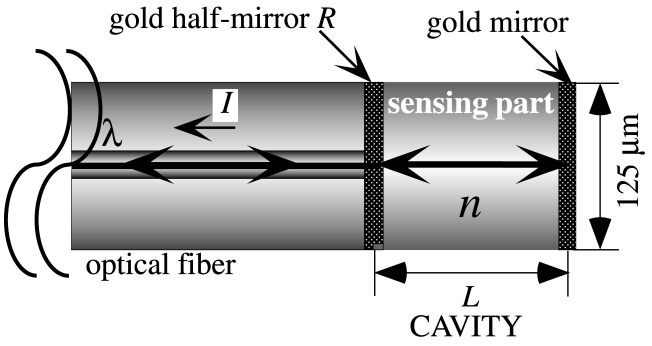

Fig. 1. Construction of the proposed probe. n, refractive index of the cavity; L, length of the cavity; R, reflectivity of the half-mirror; I, reflected light intensity; λ, wavelength of the incident light.

deformation. The latter is known from the Fabry-Perot equation. We define the dynamic range of the microprobe to be the region from the bottom of a resonance dip where the reflectivity is 70% of the dip's depth. Then, the dynamic range is expressed as

$$\Delta p = \left(\frac{\Delta p}{\Delta(nL)}\right)\frac{\lambda}{2\pi}\sin^{-1}\sqrt{\frac{0.7}{1+0.3F}}. \qquad (3.2)$$

3.2 Mechanical deformation

The optical path change with respect to the acoustic pressure change $\Delta(nL)/\Delta p$ is rewritten by the change of geometrical length $\Delta L/\Delta p$ and the change of refractive index $\Delta n/\Delta p$,

$$\frac{\Delta(nL)}{\Delta p} = nL\left(\frac{1}{L}\frac{\Delta L}{\Delta p}+\frac{1}{n}\frac{\Delta n}{\Delta p}\right). \qquad (3.3)$$

First, $\Delta L/\Delta p$ is calculated. Because the soft polymer cavity is mechanically connected to the hard silica fiber, the deformation by the pressure is not as simple as uniaxial or bulk compression of a uniform material, as shown in Fig. 2(a). Then, we employed FEM for the calculation. Here, it is assumed that the cavity is connected by a silica fiber which has approximately semi-finite length. The uniaxial deformation model that the deformation ΔL was caused by a static pressure Δp applied to the cross-sectional surface of sensor end was assumed. In the case of hydrostatic and FEM models, ΔL is derived by applying a static pressure Δp onto the entire surface of the cavity. From the results in Fig. 2(b), it is found that the FEM results have a weak dependence on the cavity length L and the hydrostatic model is not a bad approximation. The error rates of the uniaxial model and the hydrostatic model are about 200% and 8.4%, respectively. Also, the change of refractive index with respect to sound pressure $\Delta n/(n\Delta p)$ is expressed as the relationship between density and refractive index, $\Delta\rho/\rho = \Delta n/(n-1)$.[5)]

$$\frac{1}{n}\frac{\Delta n}{\Delta p} = -\frac{\Delta n}{n}\frac{\rho}{\kappa\Delta\rho} = -\frac{n-1}{n\kappa} \qquad (3.4)$$

Here, κ is the bulk modulus (polymer, 4×10^9 Pa; silica, 3.7×10^{10} Pa). The change of refractivity may cancel the change of cavity length since they have opposite signs. However, in the case that cavity material is polymer resin, the change of refractivity is much smaller than that of cavity length, as shown in Table I. Therefore polymer is a better cavity material than silica from the viewpoint of sensitivity.

3.3 Optical sensitivity

The pressure sensitivity with respect to the deformation of the cavity $\Delta G_R/\Delta(nL)$ is derived from the derivative of eq. (2.1),

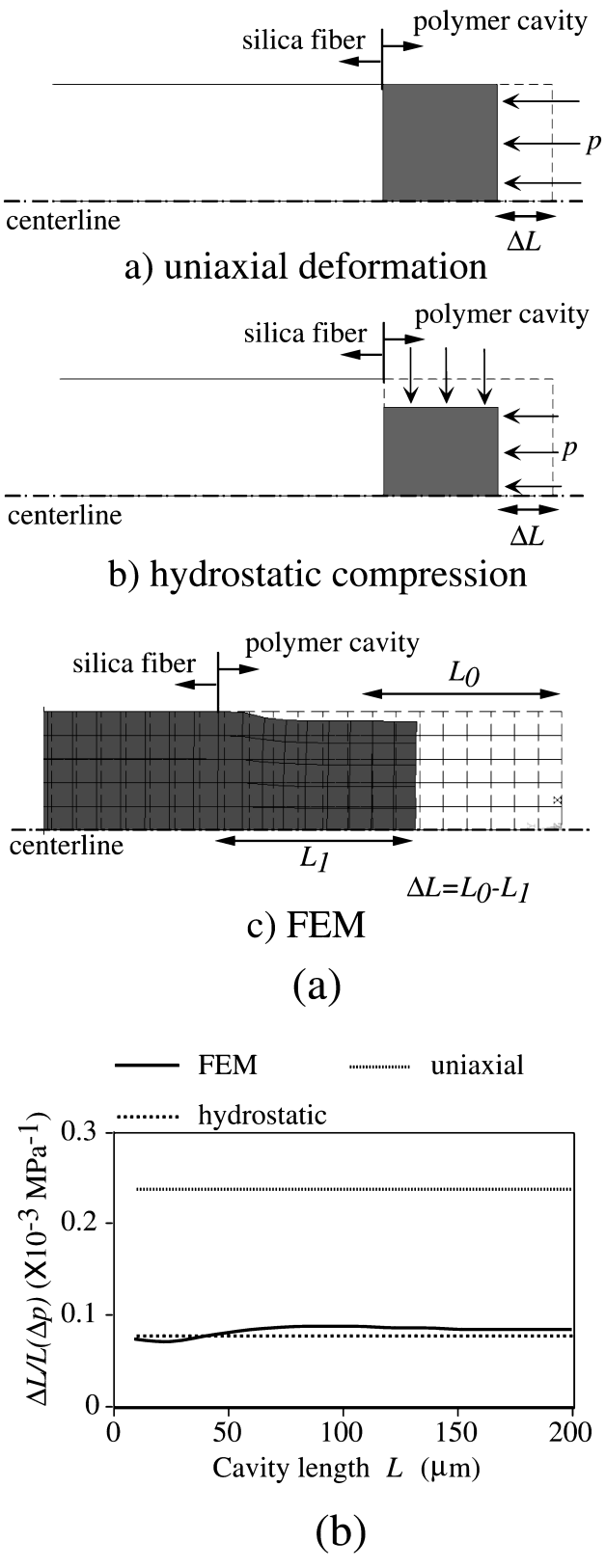

Fig. 2. (a) Deformation models of cavity. (b) Calculated deformation.

Table I. The analysis of deformation ΔL and change of refractivity Δn with respect to sound pressure Δp.

	ΔL (uniaxial)	ΔL (hydrostatic)	ΔL (FEM)	Δn
polyester resin on silica	2.38×10^{-4}	7.62×10^{-5}	$(7.21\text{–}8.56)\times10^{-5}$	-1.38×10^{-5}
silica on silica	1.37×10^{-5}	9.04×10^{-6}	$(8.78\text{–}8.95)\times10^{-6}$	-3.23×10^{-6}

$$\frac{dG_R}{d(nL)} = \frac{(1-R)(1-G_s^2)\cdot\dfrac{8\pi\sqrt{R}G_s}{\lambda}\sin\dfrac{4\pi nL}{\lambda}}{\left((1-\sqrt{R}G_s)^2+4\sqrt{R}G_s\sin^2\dfrac{2\pi nL}{\lambda}\right)^2}. \quad (3.5)$$

It is found that $\Delta G_R/\Delta(nL)$ can be determined by controlling the reflectivity of the half-mirror R and the single-pass gain G_s. L is adjusted by a precise positioning system in the fabrication procedure, while R is changed by the deposition time. However, a method of controlling the G_s of this cavity has not yet been developed. Because this cavity is not an optical waveguide with confinement, and the optical beam is widely distributed, G_s depends considerably on L. We calculated G_s by the ray tracing method. We used a face-to-face model instead of the reflection model for both calculation and experiment. Polyester resin without hardening liquid, which is the same as the material of the proposed sensing cavity, was injected between the two fibers to simulate the sensing cavity and make the reflection at the fiber end small. Two types of single-mode silica fiber with two different characteristics were used. One of them is an optical fiber which is designed to work as a single-mode fiber at the 1.3 μm band. It has a core diameter of 10 μm and a numerical aperture (NA) of 0.11. However, in this experiments, LP_{02} or LP_{21} mode might be excited since the normalized frequency V is 4.402 for the light wavelength used. Another type of single-mode fiber is a real single-mode fiber (Newport Corp.; F-SF-C-OPT) for the wavelength used in the experiment ($V < 2.406$ at $\lambda = 785$ nm). It has a core diameter of 4 μm and a *NA* of 0.11. The experimental and theoretical data agree with each other, as shown in Fig. 3. From the discussion above, it is found that $\Delta G_R/\Delta(nL)$ can be determined by L and R.

3.4 Experimental and theoretical results

Figure 4 shows the experimental setup for all the following experiments. First, to confirm cavity operation, the reflected light intensity I_0 of the cavity to the change of wavelength λ was measured. Simultaneously, we measured the ultrasonic component v_s by applying anultrasonic field of 68 kHz on the sensing part at various optical wavelengths. I_0 and v_s were extracted from the PD output by electric filters. An external cavity tunable LD (Environmental Optical Sensors, Inc.; 2010) was employed as the light source, whose center wavelength and wavelength span were 785 nm and $\pm$5 nm, respectively. These experiments were performed on a single-mode fiber for the 1.3 μm band and a real single-mode fiber mentioned in §3.3. Figure 5 shows experimental and calculated results of the reflectivity G_R on the single-mode fiber for the 1.3 μm band. By fitting the measured data into eq. (2.1), R, G_s and L of prototype probes are found to be 0.8, 0.93 and 94.2 μm, respectively.The ultrasonic component v_s, which corresponds to the sound pressure detected by the fiber probe, is plotted as a function of light wavelength in Fig. 6 as well as the calculation using eq. (3.5). As we expected, the proposed sensor is sensitive to the acoustic fields if the optical wavelength is tuned at the slope of the cavity resonances, and it is proportional to eq. (3.5). The sensitivity to sound pressure becomes zero exactly at the bottom of the resonance curve in Fig. 5. Table II shows the specifications of the prototypes used in the experiments of pressure sensitivity and dynamic range. Figure 7 shows the calculated and experimental pressure sensitivity $\Delta G_R/\Delta p$. For both cases of $V = 4.402$ and $V < 2.406$, the error between the experimental data and theoretical data was less than 10%. It should also be noted that there is a preferable region of the cavity length for building an array sensor with the wavelength division mul-

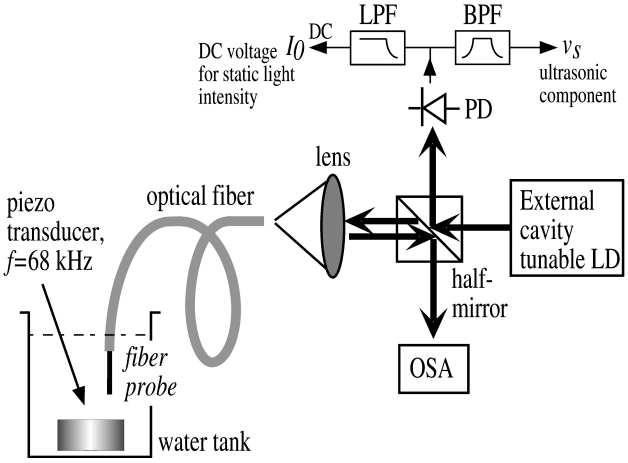

Fig. 4. Experimental setup for ultrasonic field measurements by the proposed probe.

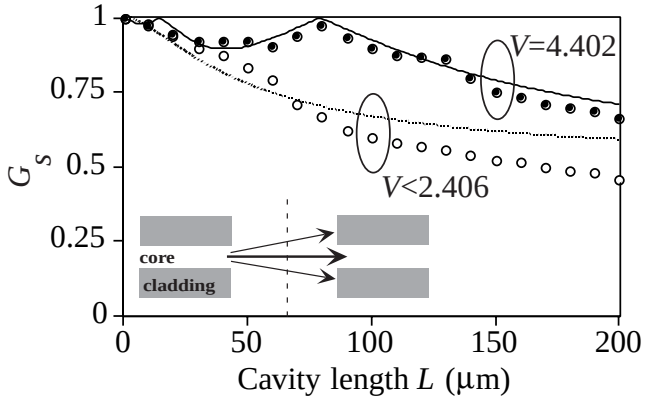

Fig. 3. Measured and calculated single-pass gain G_s as a function of cavity length L. Solid curve, dots, dotted curve and circles were calculated data for $V = 4.402$, measured data for $V = 4.402$, calculated data for $V < 2.406$ and measured data for $V < 2.406$, respectively.

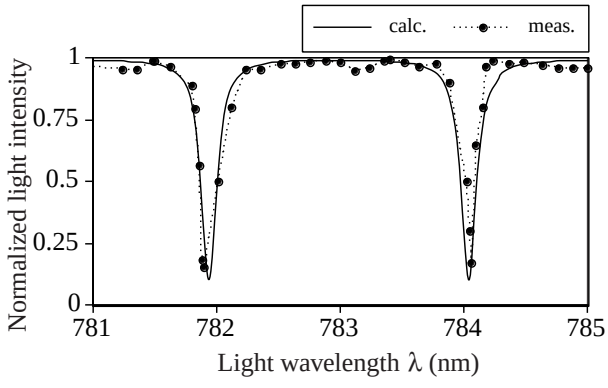

Fig. 5. Reflectance of the cavity as a function of wavelength. The measured data are plotted by - -o- -; the solid curve was calculated using eq. (2.1).

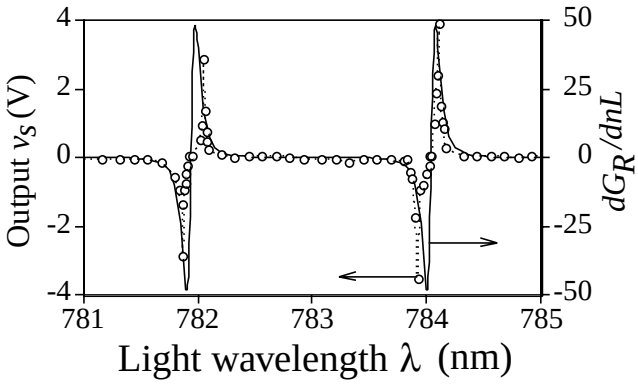

Fig. 6. Pressure sensitivity of the cavity as a function of wavelength. The measured data are plotted by - -○- -; the solid curve was calculated using eq. (3.5).

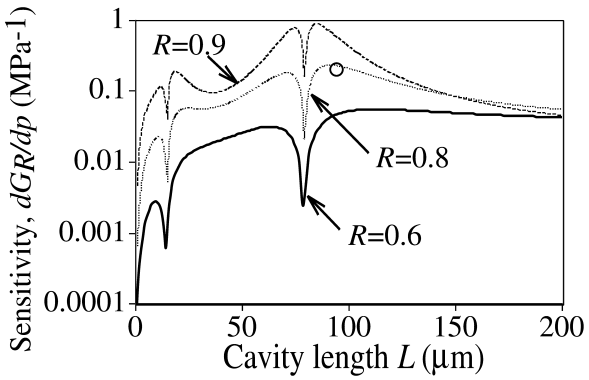

(a)

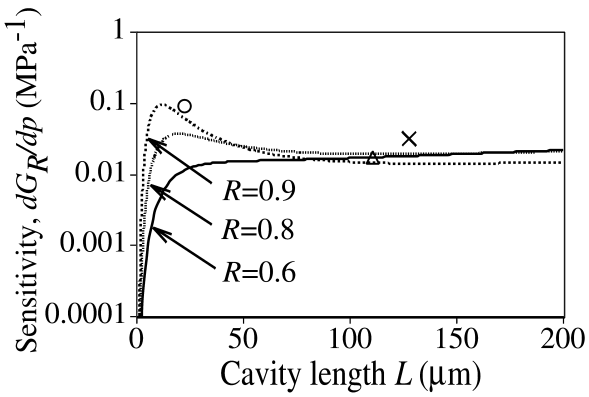

(b)

Fig. 7. Measured and calculated sensitivity of the proposed probe as a function of L. (a) Calculated and experimental results of MM1. The measured data are plotted by ◯. (b) Calculated and experimental results of SM1-3. The measured data of SM1-3 are plotted by ◯, △ and ×, respectively.

tiplexing (WDM) technique[3] since the pressure sensitivity is not change by the cavity length at that region. For example, in the region of $L > 100\,\mu$m in Fig. 7(a) and $L > 50\,\mu$m in Fig. 7(b), the sensitivity has weak dependence on L. Figure 8 shows the calculated and experimental dynamic ranges. The experimental data were 1/2–4/5 the values obtained theoretically. This difference may be caused by the drift of the operation wavelength due to the fluctuation of cavity resonance.

Table II. Specifications of the prototypes.

	MM1	SM1	SM2	SM3
R	0.8	0.62	0.6	0.85
L (μm)	94	22	111	128
G_s	0.93	0.90	0.65	0.64
λ (nm)	784.10	784.52	784.92	785.32
V, mode	4.402, LP_{02}		< 2.406, LP_{01}	

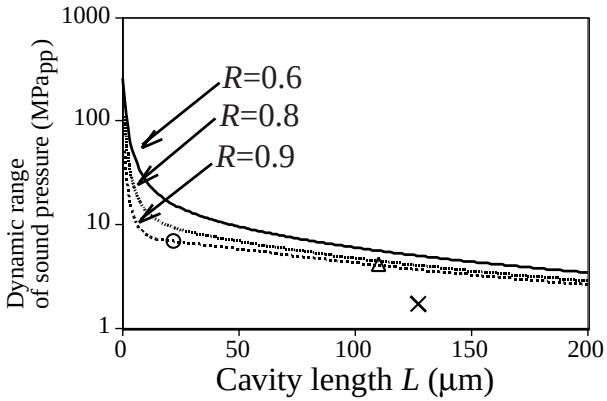

Fig. 8. Measured and calculated dynamic range of the proposed probe as a function of L. Calculated and experimental results of SM1-3. The measured data of SM1-3 are plotted by ◯, △ and ×, respectively.

4. Conclusions

The analysis of sound pressure sensitivity and dynamic range of the optical fiber microprobe was performed using the Fabry-Perot theory and FEM. Deformation of the microcavity by pressure can be approximated by a simple bulk compression model. We also obtained an appropriate cavity length in which the sensitivity variation due to cavity length change is minimized. This theory is useful for building a microprobe array with the WDM technique.

Acknowledgement

This study was partly supported by Grant-in-Aid for COE Research from the Ministry of Education, Science, Sports and Culture (#07CE2003, ÒUltra-parallel Optoelectronics).

1) P. C. Beard and T. N. Mill: Electron. Lett. **33** (1997) 801.
2) Y. Uno and K. Nakamura: Trans. IEE Jpn. **118-E** (1998) 487.
3) Y. Uno and K. Nakamura: Proc. IEEE Int. Ultrasonics Symp., Sendai, 1998 (1998) II-2.
4) T. Mukai and Y. Yamamoto: IEEE J. Quantum Electron. **17** (1981) 1028.
5) J. Stardenraus and W. Eisenmenger: Ultrasonics **31** (1993) 267.